New Phytologist

Leaf economics and plant hydraulics drive leaf/wood area ratios

Journal:	*New Phytologist*
Manuscript ID	Draft
Manuscript Type:	MS - Regular Manuscript
Date Submitted by the Author:	n/a
Complete List of Authors:	Mencuccini, Maurizio; CREAF, Universidad Autonoma de Barcelona, c/o, CREAF; Pg. Lluís Companys 23, ICREA Rosas, Teresa; Universitat Autonoma de Barcelona, Biologia Animal, Vegetal i Ecologia; CREAF, Centre de Recerca Ecologica i Aplicacions Forestals Rowland, Lucy; University of Exeter, Department of Geography Choat, Brendan; University of Western Sydney, Hawkesbury Institute for the Environment Cornelissen, Johannes (Hans); University Amsterdam, Department of Systems Ecology Jansen, Steven; Ulm University, Institute for Systematic Botany and Ecology Kramer, Koen; Wageningen University and Research Wageningen Environmental Research, Forest Ecology and Forest Management Group Lepenas, Andrei; University at Albany State University of New York, Geography and Planning Manzoni, Stefano; Stockholms Universitet, Institutionen för naturgeografi ; Stockholm University, Bolin Centre for Climate Research Niinemets, Ülo; Estonian University of Life Sciences, Institute of Agricultural and Environmental Sciences; Estonian Academy of Sciences, Biology Reich, Peter; University of Minnesota, Department of Forest Resources Schrodt, Franziska; University of Nottingham, Geography Soudzilovskaia, Nadia; Leiden University, Institute of Environmental Sciences, CML Wright, Ian; Macquarie University, Biological Sciences;
Key Words:	Huber value, xylem hydraulics, leaf economics spectrum, wood density, leaf size, Corner's rules, biomechanics, trait tradeoff

Leaf economics and plant hydraulics drive leaf/wood area ratios

M Mencuccini[1,2*], T Rosas[1,3], L Rowland[4], B Choat[5], JHC Cornelissen[6], S Jansen[7], K Kramer[8], A Lepenas[9], S Manzoni[10,11], Ü Niinemets[12,13], P Reich[5,14], F Schrodt[15], NA Soudzilovskaia[16], I Wright[17], J Martínez-Vilalta[1,3]

[1] CREAF, E08193 Bellaterra, Barcelona, Spain

[2] ICREA, Pg. Lluís Companys 23, 08010 Barcelona (Spain).

[3] Universitat Autònoma de Barcelona, E08193 Bellaterra, Barcelona, Spain

[4] Department of Geography, College of Life and Environmental Sciences, University of Exeter, Exeter, UK

[5] Hawkesbury Institute for the Environment, Western Sydney University, Locked Bag 1797 Penrith 2751 NSW, Australia

[6] Systems Ecology, Department of Ecological Science, Vrije Universiteit, De Boelelaan 1081, 1081 HV Amsterdam, The Netherlands

[7] Ulm University, Institute of Systematic Botany and Ecology, Albert-Einstein-Allee 11, 89081 Ulm, Germany

[8] Wageningen University and Research, Droevendaalsesteeg 1, 6700 AA, Wageningen, The Netherlands

[9] Department of Geography, New York State University at Albany, Albany, NY, USA

[10] Physical Geography, Stockholm University, Stockholm, Sweden

[11] Bolin Centre for Climate Research, Stockholm University, Stockholm, Sweden

[12] Estonian University of Life Science, Kreutzwladi 1, 51006 Tartu, Estonia

[13] Estonian Academy of Sciences, Kohtu 6, 10130 Tallinn, Estonia

[14] Department of Forest Resources, University of Minnesota, St. Paul, MN 55108 USA

[15] School of Geography, University of Nottingham, Nottingham, UK

[16] Institute of Environmental Sciences, CML, Leiden University; Einsteinweg 2, 2333 CC Leiden, The Netherlands

[17] Department of Biological Sciences, Macquarie University, Sydney NSW 2109, Australia

*corresponding author.

Maurizio Mencuccini

CREAF, Universidad Autonoma de Barcelona
Cerdanyola del Valles 08193
(Barcelona, Spain)
m.mencuccini@creaf.uab.cat
tel. +34-93-5868474
fax +34-93-5814151

Contributions by authors:

MM, TR, JM-V and BC conceived and implemented the research; all authors contributed to data collection; MM analyzed the data with JM-V, BC and TR; MM wrote the first draft with contributions from TR, JM-V, IW; all coauthors contributed substantially to revisions.

Keywords: Huber value, xylem hydraulics, leaf economics spectrum, wood density, leaf size, Corner's rules, biomechanics, trait tradeoff

RUNNING TITLE: Global drivers of leaf/wood area partitioning

Total word count (excluding summary, references and legends):	**6,491**	No. of figures:	**3**
Summary:	**200 (max 200)**	No. of Tables:	**1**
Introduction:	**1,104**	No of Supporting Information files:	**Methods S1, Table S1 to S3, Figure S1 to S5.**
Materials and Methods:	**2,122**	No. of references	**99**
Results:	**1,083**		
Discussion:	**2,182**		
Acknowledgements:	**114**		

Abstract

Biomass and area ratios between leaves, stems and roots regulate many physiological and ecological processes. The Huber value H_v (sapwood area/leaf area ratio) is a central variable controlling plant water balance and its drought responses, but it currently cannot be predicted based on easily measurable and widely available traits.

We hypothesise that global patterns in H_v of terminal woody branches can be predicted based on variables related to plant hydraulics, leaf economics and leaf size.

Using a global compilation of 1135 species-averaged H_v, we show that H_v decreases with specific leaf area, leaf mass, xylem hydraulic specific conductivity K_s, wood density and plant stature. All traits depend on climate but the climatic correlations are stronger for explanatory traits than H_v. Negative isometry is found between H_v and K_s, suggesting a compensation to maintain hydraulic supply to leaves across species. High H_v and low K_s are seen in short small-leaved low-SLA shrubs in arid relative to tall large-leaved high-SLA trees in moist environments.

This work identifies the major global drivers of branch sapwood/leaf area ratios. Our approach based on widely available traits facilitates the development of accurate models of aboveground biomass partitioning and helps improve predictions of vegetation responses to drought.

Introduction

Plant growth and survival depend in large part on the characteristics of individual plant organs and on the partitioning of resources to these organs (Thornley 1972; Grime 1979; Tilman 1988; Westoby 1998). Hence, biomass partitioning integrates key physiological and ecological processes (Hunt & Cornelissen 1997; Shipley 2006; Poorter *et al.* 2015). At the global scale, the biomass ratios between leaves, stems and roots are known to be affected by abiotic factors such as temperature (Gill & Jackson, 2000; Lapenis et al., 2005; Reich *et al.*, 2014a; Reich *et al.*, 2014b; Freschet et al., 2017), light (Poorter *et al.* 2012), potential evapotranspiration (Ledo *et al.* 2017), soil water stress (Lapenis *et al.*, 2005; Poorter *et al.*, 2012) and nutrients (Poorter *et al.* 2012; Freschet *et al.* 2017), and biotic factors such as plant size (Poorter *et al.* 2015; Ledo *et al.* 2017). Biomass ratios globally have also been reported to vary by plant functional type, e.g., eudicots invest more in leaf tissues than monocots and gymnosperms more than angiosperms (Poorter *et al.* 2012; Duursma & Falster 2016). While global patterns in biomass ratios are beginning to be elucidated, the dependence of partitioning among tissues on specific traits is not well understood.

Functional balance and adaptive dynamics theories (Thornley 1972; Bloom *et al.* 1985; Franklin *et al.* 2012; Farrior *et al.* 2013) suggest that, over evolutionary time scales, partitioning should be regulated to guarantee access to the most limiting resource in competitive and variable environments. However, complications arise because plant size declines with reduced resource availability (Coleman *et al.* 1994; McCarthy & Enquist 2007), biomass partitioning varies with plant size (Enquist & Niklas 2002; Poorter *et al.* 2015), and because biomass ratios reflect both partitioning and turnover times (Thornley 1972; Gill & Jackson 2000; Reich 2002; Niinemets 2010). Additionally, hydraulic (Tyree & Ewers 1991) and biomechanical (Niklas & Spatz 2010) properties of stems depend on stem cross-sectional areas and their geometry. If the objective is to derive predictive relationships of tissue partitioning, areal ratios of leaves and xylem may be more appropriate than mass ratios. Finally, linking partitioning to plant trait spectra is difficult, because of the many constraints that need to be considered simultaneously (Dewar *et al.*, 2009; Franklin *et al.*, 2012). One study (Duursma & Falster 2016), showed that biomass distribution between stem and leaves across tree functional types varied with plant size and specific leaf area (*SLA*), suggesting that the partitioning of biomass between organs may depend on plant and leaf properties. It then follows that patterns of partitioning may be tightly linked to the trade-offs controlling the functional properties of those organs, which in turn are dependent on climate and resource availability.

The need to build sufficient xylem hydraulic capacity to supply the canopy, given a certain distance between roots and leaves (Zimmermann 1983; Tyree & Ewers 1991) provides a first

constraint, i.e., higher hydraulic efficiency (i.e., higher specific conductivity per unit xylem area, K_s) may be required for thin and long stems to compensate pressure losses along a longer hydraulic pathway. A second trade-off comes from Corner's rules (Corner 1949). Corner's rules state that larger individual leaves are subtended by thicker stems and are more widely spaced in branches of a given length, implying that for a given leaf area, the trade-offs between building many small leaves or few large ones have consequences for stem size (Westoby & Wright 2003; Kleiman & Aarssen 2007; Olson *et al.* 2009; Smith *et al.* 2017). A third trade-off relates to the partitioning towards leaf area construction in relation to the carbon returned by photosynthesis over a leaf's lifespan (Kikuzawa 1991), as embodied in the leaf economics spectrum (LES) theory (Reich *et al.* 1997; Wright *et al.* 2004; Shipley *et al.* 2006). The central trait mediating this trade-off is *SLA*, which is the ratio between the radiation-intercepting leaf area and the required mass investment (Niinemets 1999, 2001). Finally, one might expect wood density (*WD*) to control the amount of biomass investment in xylem cross-sectional areas. High *WD* increases mechanical stiffness and resistance to breakage (Niklas & Spatz 2006; Chave *et al.* 2009) and cavitation (Hacke *et al.* 2001) but high *WD* also implies high carbon cost, especially for tall trees (Mencuccini 2003). Based on mechanical stability and carbon cost principles, the trade-offs between building thin terminal branches with dense wood or building thick branches with low density (Niklas & Spatz 2010) may have consequences for the ratios between xylem and leaf areas.

To advance our understanding of how xylem hydraulics, wood and leaf economics may control resource partitioning in woody plants globally, we employ the Huber ratio (xylem sapwood area / leaf area, H_v) of crown-top branches as a measure of the relative areal ratios of leaves and wood (Tyree & Ewers 1991). H_v can be viewed as the ratio of investment in xylem area (i.e., excluding pith, heartwood, stem bark and phloem) over the expected gains obtained by leaf display and thus, it is an essential parameter in models of water use by vegetation (Mencuccini *et al.* 2019). It is employed to convert xylem specific conductivity into a more physiologically meaningful variable, i.e., leaf-specific conductivity ($K_L = K_s H_v$). K_L links the unit-area water flux through plants with the water potential gradient necessary to drive that flux. While Corner's rules do not distinguish between the components of branch cross-sectional area, H_v only considers tissues potentially involved in water transport. Relative to a pipe model ratio, the H_v indicates investment for hydraulic supply to leaves, while biomechanical support and storage functions are not considered. Because H_v is defined based on actively-conducting sapwood, turnover times of sapwood into heartwood are implicitly considered. Although H_v can vary somewhat within a plant depending on where it is measured (cf., review in Mencuccini *et al.* 2019), the dataset reported here refers to samples of

crown-top terminal branches. Finally, we develop an analytical framework to predict H_v from organ-level traits.

Specifically, we test the hypotheses that the relative partitioning between sapwood area and leaf area (H_v) is affected jointly by properties controlling leaf economics and plant hydraulics, i.e., by a) leaf traits broadly related to leaf spectra (as defined by the *SLA* and leaf size) and b) xylem hydraulic efficiency K_s and maximum tree height H_{max} (which is strongly related to maximum hydraulic path length). Additionally, we also test a hypothesis related to wood economics, i.e., that c) *WD* scales with H_v. Understanding how partitioning between leaves and wood in terminal branches is jointly determined by leaf and wood properties is a significant step towards predicting how organ-level traits can affect global patterns of biomass partitioning and vegetation responses to drought.

Materials and Methods

Theory

A theoretical model to predict H_v ($cm^2\ m^{-2}$) based on organ-level traits is currently not available. As a starting point, we employ the definition of the Huber value to partition the identity into component variables:

$$H_v = \frac{A_x}{A_{L,tot}} = \frac{A_x}{\sum A_L} = \frac{A_x}{\sum SLA\ M_L} = \frac{A_x}{SLA\ n\ M_L}, \quad \text{(Eqn. 1)}$$

where A_x and $A_{L,tot}$ are xylem sapwood area (cm^2) and subtended leaf area (m^2), respectively. The capital sigma in the denominator indicates a summation over all leaves of a crown-top twig, A_L, M_L and *SLA* are mean area of a leaf (m^2), mean mass of a leaf (10^{-3} kg) and mean specific leaf area ($m^2\ kg^{-1}$), respectively, while *n* is the number of leaves in a branch of a given length. SLA is known to depend on light availability within tree crowns (e.g., Niinemets *et al.* 2015), while H_v data reflects only conditions of canopy-top branches. Once variables are log-transformed, Eqn. 1 predicts a negative scaling for H_v against both M_L and *SLA*. In practice, negative isometric scaling (b=-1.00) is not expected between these variables, because of, among other factors, non-zero covariances between M_L and *SLA* and between M_L and *n*. *SLA* and M_L act very distinctively with regard to how they might affect H_v. Doubling *SLA* halves H_v without changes in leaf biomass. Conversely, doubling M_L halves H_v by doubling leaf biomass. The presence of A_x in the numerator of Eqn.1 suggests a size-dependency of H_v. To incorporate it, the potential hydraulic conductance of a plant can be expressed

as K_p = K_s A_x/H_{max}, where K_p (kg MPa^{-1} s^{-1}), K_s (kg m^{-1} MPa^{-1} s^{-1}) and H_{max} (m) are potential plant hydraulic conductance, branch specific conductivity and plant maximum height, respectively. This conductance is referred to as 'potential' because it does not account for actual path length, only maximum height. We employ H_{max} instead of actual sampling heights, because sampling heights are not available for the majority of our samples. Hence our results must be understood with regard to the effects of plant potential stature, not actual height *per se*, on these relationships. We recognise that metabolic scaling theory (MST, West *et al.* 1999; Savage *et al.* 2010) provides suitable expressions for this scaling. We do not employ quarter-power relationships, as our intention is not to test our global dataset against predictions from MST, but to explore the joint covariation of leaf economics and xylem economics variables in relation to H_v. Substituting K_p H_{max} /K_s for A_x into Eqn.1 gives:

$$H_v = \frac{K_p \quad H_{max}}{n\ SLA\ K_s\ M_L} \qquad \text{(Eqn.2)}$$

The first term on the right hand side of the equation contains the ratio K_p/n, the total stem hydraulic supply capacity to each leaf. Both K_p and n are dependent on stem diameter (Mencuccini 2002; Savage *et al.* 2010; Smith *et al.* 2017), while K_p/n is much less so (West *et al.* 1999). The second term on the right hand side of Eqn. 2 predicts a direct scaling of H_v with H_{max} and an inverse scaling with K_s, *SLA* and M_L. The direct scaling of H_v with H_{max} ensures that taller plants have greater relative allocation to xylem area to compensate for their stature (McDowell *et al.* 2002). This compensation is moderated by other processes, i.e., vertical conduit tapering (West *et al.* 1999; Anfodillo *et al.* 2006) and larger conduits at the apex of tall plants (Olson *et al.* 2014, 2018), both of which affect K_s. An inverse scaling of H_v with H_{max} may thus also be obtained, if K_s scaled with H_{max} more than proportionally. In addition, a negative scaling with H_{max} may also be obtained if plants minimise sapwood construction and/or maintenance costs, instead of hydraulic resistance (Anfodillo *et al.* 2016; Fajardo *et al.* 2019). An inverse relationship between H_v and K_s is expected because of functional balance between water supply and demand (Whitehead & Jarvis, 1981; see derivation in the Supplementary Information, Methods S1) and it has been found empirically before for smaller datasets (Choat *et al.* 2011; Gleason *et al.* 2012).

Equations 1-2 express H_v in term of the constituent traits, thus providing a predictive reference framework for tissue partitioning based on organ-specific traits. Beside the predictions based on the framework above, additional models were tested. Firstly, we tested whether H_v scaled with *WD* (strictly, stem specific gravity). A negative relationship between H_v and *WD* may arise because of xylem carbon construction costs (cf., Supplementary Materials Section S1 for in-depth

discussion). Secondly, we tested a model excluding K_s from the set of traits employed to predict H_v. The advantage of excluding K_s is that it allows to obtain a model for H_v based only on widely available easy-to-measure traits, making it possible to employ global databases to predict sapwood-leaf area ratios. Overall, our analyses provide the first approximation to a framework explaining the variability in a difficult-to-predict allocation trait, based on standard leaf and xylem traits and plant stature.

Datasets

Measured values of crown-top branch H_v were obtained from a) an updated version of the hydraulic dataset by Choat *et al.* (2012) (i.e., XFT, xylem functional traits), including several new datasets from China, b) an Amazonian dataset from RAINFOR (Patiño *et al.* 2012), c) an Australian dataset (from Togashi *et al.* 2015) and d) an African/S. American dataset from TROBIT (Schrodt *et al.* 2015). Smaller datasets from China were obtained from (Niu *et al.*, 2017; Song *et al.*, 2018). The geographical distribution of sampling sites/species location is given in Fig.S1 and the biome distribution plot in Fig. S2. The RAINFOR and the TROBIT projects (accounting for ~50% of all H_v here) followed a single protocol for the measurement of leaf area, mass, xylem area, *SLA* and wood density (Patiño 2005). Specifically, 1-m-long top-canopy branches were sampled typically at the end of the rainy season (leaf phenology can be variable and is poorly predictable in the tropics, e.g., Wu *et al.*, 2016) from sun-exposed crowns of trees of diameter at breast height >10cm. Bark, heartwood if present, and xylem pith were visually excluded from xylem measurements. However, since dyes were not routinely used, hydraulically active xylem was not identified. For the hydraulic dataset (~50% of the entries), crown top samples were also typically collected. Units and protocols were checked by experts, although study-to-study variability in sampling/measurement methods may be present in our sample (especially, regarding use of dyes and sample length). Measurements conducted on seedlings, inside greenhouses and those subjected to experimental treatments were excluded from this study. Values of wood specific conductivity K_s were obtained from the updated XFT, leaf economics traits (*SLA*, leaf lifespan LL), H_{max} and *WD* from XFT and Glopnet (Wright *et al.* 2004), (Patiño *et al.* 2012), (Schrodt *et al.* 2015) and/or TRY (Kattge *et al.*, 2011). Xylem vulnerability to embolism from XFT was employed for one analysis, for which r-shaped curves were excluded. Individual, one-sided projected leaf areas A_L were obtained from (Wright *et al.* 2017) and leaf masses M_L calculated by dividing A_L by *SLA*.

Information on genus-level woodiness, leaf habit, leaf type, leaf shape and plant growth form were obtained from the sources above or from (Zanne *et al.* 2014). When required, missing pieces of information were extracted by web scraping of wiki pages from Wikipedia (https://en.wikipedia.org/wiki/Main_Page), Encyclopaedia of Life (http://eol.org/), Flora of China (http://www.efloras.org) and Useful Tropical Plants (http://tropical.theferns.info/) using *xml2*, *rvest* and *httr* in R (R Core Team 2017). The dataset was finally trimmed to the following levels for each categorical variable: woodiness (woody only), leaf habit (winter and drought-deciduous, evergreen), leaf shape (compound, simple), leaf type (needle leaf, broadleaf), plant habit (shrub, tree) and taxon group (Angiosperm, Gymnosperm). The final dataset contained 1135 species-averaged H_v values from 736 sites (1618 unique values when including lianas, vines, succulents and cacti). The other quantitative variables had somewhat lower coverage (i.e., >90% for *SLA* and *WD*, >70% for H_{max} and leaf size, 40% for K_s).

For each species record, species climatic envelopes were calculated with *speciesmap* (https://remkoduursma.github.io/speciesmap/articles/Using_speciesmap.html), an R package that combines species occurrences from GBIF (Global Biodiversity Information Facility, http://www.gbif.org), with climate layers from WorldClim (http://www.worldclim.org) and CGIAR-CSI, cf. Trabucco *et al.*, 2008). *speciesmap* rasterizes species occurrences and extracts 0.025, 0.5 and 0.975 quantiles for mean annual temperature (MAT), precipitation (MAP) and potential evapotranspiration (PET) across all grid cells of the species occurrence region. Converting the occurrence data into presence/absence grid cells equally weighs over- and under-sampled areas in the climate envelope estimates. Species classification into biomes was obtained from a Whittaker diagram of MAT and MAP (Wright *et al.* 2004). For those H_v measurements where Latitude/Longitude were available from the original publications, we compared MAT/MAP at the sampling site against values obtained for the GBIF climate envelope (slope=0.96, R^2=0.94, n=686, and slope=0.90, R^2=0.91, n=686, for MAT and MAP, respectively; the slopes <1.0 suggest, as expected, a 4-10% underestimation of MAT/MAP from GBIF relative to local values). Because annual MAP/MAT values may be poorly related to relative water supply particularly during the growing season, a Moisture index (MI) was calculated as MAP/PET. To bring species binomials to a common taxonomy, names were matched against accepted names in The Plant List using *taxonstand* (Cayuela *et al.* 2012). Any binomials not found in this list were matched against the International Plant Names Index (IPNI; http:// www.ipni.org/), eFloras and Tropicos (http://www.tropicos.org). The final list with unresolved species nomenclature was carefully checked manually.

Statistical analyses

To assess functional scaling between variables, bivariate relationships between H_v and other traits (*SLA*, M_L, K_s, H_{max} and *WD*) were summarised using standardised major axis (SMA) slopes using *smatr* (Warton *et al.* 2006). All traits were log-10 transformed to improve residual distribution and examine relationships across order of magnitude differences. We carried out a goodness-of-fit test for the overall relationships to identify global scaling patterns (i.e., overall line slopes and intercepts ±95% confidence intervals). Slopes were compared between categorical groupings by leaf type (broad/needle leaves), leaf shape (simple/compound) leaf habit (winter deciduous/drought deciduous/evergreen), plant growth form (shrub/tree) and taxon group (Angiosperm/Gymnosperm) using a likelihood ratio test (Warton *et al.* 2006). Where slopes were deemed not to significantly differ, we tested for intercept differences between the common-slope lines and/or shifts of the data clouds along the common-slope line using a Wald test with one degree of freedom (Warton *et al.* 2006).

Path models (SEM) were used to examine whether the hypothesised correlation structures were consistent with the observed multivariate relationships among traits determining H_v. We used the sem function in *lavaan* (Rosseel 2012) and followed Brown (2006) for model selection and diagnostics. *SLA*, M_L, H_{max} (in some models also *WD* and/or K_s) were allowed to co-vary with each other as they jointly affected H_v. To explore the possibility that these relationships were modulated by additional factors, we allowed for trait covariance to depend on additional categorical variables (i.e., leaf shape, leaf type, plant growth form and taxon group), included as fixed effects in some models. Directed climate effects (MAT, MAP, MI) on leaf, xylem traits and H_{max} were included in some models, together with directed climate effects on H_v. The saturated path models were simplified by removing non-significant paths (using z tests and ΔAIC values) until a minimal adequate model was found. Goodness of fit was assessed using absolute fit, parsimony and comparative fit (Brown 2006). Full-information Maximum Likelihood allowed including species with partially missing traits. Finally, the path model coefficients were used to predict H_v based on organ-specific traits.

To test whether relationships of organ traits with H_v were affected by leaf turnover times, the models above were modified to include leaf lifespan LL. Also, as an alternative, we employed leaf habit (deciduous/evergreen) in some models, because the sample size for *LL* (n=105 coupled values of *LL* and H_v) was much lower than for leaf habit. Leaf habit strongly relates to *LL* (t-test, P=1.14 e^{-10}). Variation in LL is high among evergreen species, but the consequences for our interpretation are minimal because models with *LL*, leaf habit, or without are almost identical.

To check for the possibility that systematic biases were present across the original datasets (XFT; RAINFOR; TROBIT; Togashi *et al.*, 2015; Niu *et al.*, 2017; Song *et al.*, 2018), we treated these datasets as a random factor in a linear mixed model (*nlme*, Pinheiro & Bates, 2000). We modelled H_v as a function of leaf and xylem traits, by varying intercept and slope as a function of dataset. We tested the significance of the factor "dataset" by running an ANOVA comparison of the model accounting for dataset as a random factor against a simpler linear model without the random factor. The test showed that the simpler linear model was equally effective (P=0.9998). We therefore discard the possibility that systematic biases across pooled datasets can affect our conclusions, although we acknowledge that study-to-study variability within each dataset is likely. All analyses were carried out in R version 3.4.3 (R Core Team 2017).

Results

In bivariate analyses, H_v scales significantly, inversely and with similar correlation strength (r from -0.54 to -0.60) with each of the three leaf traits, i.e., *SLA*, individual leaf area A_L and individual leaf mass M_L (all P<2.2 e^{-16}, Figure 1a and b, Table 1). H_v also scales significantly and inversely with xylem specific conductivity K_s and plant stature H_{max} (r = -0.53 and r = -0.45; both P<2.2 e^{-16}). Finally, H_v and *WD* are positively but poorly related (P=0.09, r=0.06). In log10 scale, H_v varies over 3 orders of magnitude, much more than *SLA* (>1 order), slightly more than K_s and H_{max} (<3 orders), but less than leaf size (6 orders). Apart from a few gymnosperms, species with very high H_v are often short shrubs with needle-like leaves in the Proteaceae, Ericaceae, and Asteraceae of the steppes/semi-deserts of S America or Australia. Those with very low H_v tend to be large-leaved tall tropical trees in a large number of families (esp., Fabaceae and Malvaceae) in either wet or dry forests. The scaling slope of H_v against *SLA* (- 1.93) is far steeper than -1.0 (P<2.2 e^{-16}). By contrast, the scaling slopes against M_L and A_L are significantly flatter than -1.0 (b= -0.50 and -0.44, respectively; P<2.2 e^{-16}). The slopes against K_s and H_{max} are not significantly different from negative isometry (Table 1, b=-1.04 and b=-0.96, respectively).

Plant growth form (shrub/tree) and taxon group (Angiosperm/Gymnosperm) affect the magnitude but not the direction of these relationships (cf., Figure 1, Table S1). Relative to trees, shrubs are characterised by leaves with lower *SLA*, smaller A_L and M_L and by a xylem with lower K_s, while having a higher H_v (Figure 1). In contrast, Gymnosperms are shifted vertically downwards and tend to have lower H_v for a given *SLA*, leaf size and K_s relative to Angiosperms (Table S1). For a given stature, shrubs are shifted downward and Gymnosperms upward, relative to Angiosperms. When LL

is tested in bivariate relationships, it co-varies positively and significantly with H_v, but the relationship is weak (P<0.05, r=0.28). Similar results are obtained for leaf habit and H_v (P<0.01, r=0.10).

Many of the bivariate relationships between H_v, M_L, A_L, K_s, *WD*, H_{max} and *SLA* are affected by various categorical variables (Table S1). Regardless of the specific comparison, the inverse relationships between H_v and other traits are conserved, although low sample size makes the relationships non-significant for some groups (needle-like leaves, winter-deciduous plants). Generally, categorical variables related to leaf shape (simple/compound), leaf type (broad/needle leaves) and leaf habit (deciduous/evergreen) are associated with changes in the bivariate slopes between H_v and traits. Out of the possible 18 relationships, nine have heterogeneous slopes (cf., Table S1 for the P slope test values). In contrast, growth form (shrub/tree) and taxon group (Angiosperm/Gymnosperm) are only associated with elevation changes and shifts in data clouds along the common-slope lines (Tables 1 and S1).

SEM analyses (Table S2) confirmed that each of *SLA*, M_L, H_{max} and K_s contribute substantially (*SLA* > M_L > K_s > H_{max}) and independently to variation in H_v (Figure 2A). H_v remains negatively related to H_{max}, leaf (*SLA*, M_L) and xylem (K_s) properties, with this model being strongly supported (P=0.697, Table S2; Figure 2A). In this and subsequent models, substituting A_L for M_L leads to almost identical results (data not shown). All four traits strongly co-vary with one another.

We verified the robustness of the dependency of H_v against H_{max}, leaf and xylem traits, by incorporating one additional categorical variable (i.e., taxon group, plant growth form, leaf habit, leaf form, leaf shape) with effects on these traits. In no case do we find that the scaling of H_v against leaf/xylem traits disappears or is strongly altered (with the partial exception of the scaling of H_{max}, Figure S3). In all cases, the categorical variables affect the traits directly, while their effects on H_v are either very small (Fig. S3E) or non-significant (other panels in Fig. S3). Conversely, highly significant differences in H_v are always found across the levels of all these categorical variables using a general linear model (i.e., when trait effects on H_v are not accounted for; always P<0.0001; data not shown). When LL is tested with the co-varying leaf/xylem traits, it is not found to be a contributor to H_v and it is excluded (P>>0.05). Similarly, despite its much larger sample size, leaf habit is not a significant contributor to H_v (Fig.S3C).

We also explored the robustness of these relationships to differences in climatic conditions, by incorporating MAT, MAP (singly or in combination) or MI across the species climatic envelopes (MAP and MAT are highly and positively correlated in our dataset, P<2.2e^{-16}, R^2=0.48). Highly

significant effects of MAT, MAP and MI are found when tested directly in correlations against H_v ($P<2.2e^{-16}$, r=0.49; $P<2.2e^{-16}$, r=0.43, and $P<2.2e^{-16}$, r=0.28, respectively; H_v declines with increases in MAT, MAP or MI). Interestingly, when examined within the network of trait relationships explaining H_v, all four plant traits (*SLA*, M_L, H_{max} and K_s) increase at higher MAT, MAP and MI. However, direct climatic effects on H_v are comparatively small or non-existent (Figure S4). In addition, the proportions of explained variance of H_v in models with the direct effects of climate on H_v are lower than the proportions for the model without climate (i.e., r^2 = 0.48-0.50 versus 0.54, when climate is versus when it is not included, respectively; cf., Fig.2A with Fig. S4). Importantly, the path coefficients from traits to H_v change minimally up or down compared to previous models.

Having examined the relationships between H_v and H_{max}, leaf and xylem traits, *WD* is included in the path models. *WD* co-varies with all four other traits and negatively affects H_v, contributing to increase the model r^2 for H_v from 0.54 to 0.57 (Table S2, Figure 2). The direction of the effect of *WD* on H_v remains identical (and its magnitude similar), with the inclusion of additional categorical variables (data not shown). Overall among all models, the best one explains 57% of the variance in H_v (Figure S5 and Table S2).

Finally, we examined the performance of a model based only on widely available traits, i.e., excluding the trait with the lowest coverage (K_s) (Figure 3). A model based on *SLA*, M_L, H_{max} and *WD* explains almost the same amount of variance (i.e., 53%) as the one including xylem conductivity (54%) and somewhat less compared to the model with all five traits (57%, cf., Figures 2 and 3), but with comparable standardised root mean square residuals (SRMSR) (Tables S2 and S3).

Discussion

We show evidence of consistent global scaling of H_v against plant stature, leaf and wood traits, with relationships robust to the incorporation of climatic variables and major plant groupings, with the best model explaining close to 60% of the global-scale variability in H_v in a sample of >1,100 species. By comparison, a regression against MAT and MAP explains only 26% of the variance of H_v (data not shown). This result generalises findings previously reported based on smaller datasets, with relationships between H_v and/or K_s with *SLA* and/or *WD* (Stratton *et al.* 2000; Meinzer *et al.* 2004; Pickup *et al.* 2005; Gleason *et al.* 2012; Patiño *et al.* 2012), of H_v with H_{max} (Liu *et al.* 2019) and of a negative H_v-K_s relationship (Martínez-Vilalta *et al.* 2004; Choat *et al.* 2011; Togashi *et al.* 2015). Our findings can be employed to improve models' skills for the prediction of vegetation functions in

biomes where a lack of empirical data currently limits the parameterization of plant hydraulic processes.

Covariation between K_s and H_v in relation to leaf size and SLA

H_v scales against individual leaf mass M_L with a slope of ~ -0.5 (Table 1). Strictly speaking, Equation 2 predicts a scaling of -1.00, although, as explained before, additional variables may affect this slope. Given the lack of information regarding these variables at the global scale, we refrain from interpreting the discrepancy between predicted and observed exponent of this relationship. It is tempting to explain the scaling between K_s and M_L (or A_L) as a consequence of the longer path length inside longer leaves, leading to greater conduit tapering and larger K_s down the branch. Such analysis should consider the potential covariations with all the other hydraulic variables (cf., Supplementary Information Section S1 and Whitehead & Jarvis (1981)). The positive slope of K_s almost exactly matches the negative slope of H_v against M_L, effectively leading to an invariance of the product of these two variables (i.e., leaf specific hydraulic conductivity K_L, $K_L = K_s H_v$) across leaf sizes (data not shown). Changes in M_L impact on many other functional aspects, including proportion of supporting versus physiologically active tissues (Niinemets *et al.* 2007), radiation load and boundary layer conductances (Wright *et al.* 2017). Hence, it is remarkable that no trends are found in the relationship between M_L and K_L.

With regard to the H_v-*SLA* scaling, we find a much steeper slope (~ -1.9, Table 1), implying a more-than-proportional decline in H_v with *SLA*. Similar to the case above, K_s scales positively against *SLA* with a slope that is so steep (slope of ~ 1.6, Table 1) to effectively negate the negative scaling of H_v. Hence the increase of K_s with *SLA* balances the decline of H_v with *SLA*, again leading to no relationship between *SLA* and leaf-specific conductivity K_L (data not shown). Although the processes leading to these specific scaling exponents are not known, their consequences are apparent. Stomatal conductance and unit-area photosynthetic rates are positively associated with hydraulic capacity in leaves and stems (Mencuccini 2003; Brodribb *et al.* 2004; Santiago *et al.* 2004; Scoffoni *et al.* 2016). Globally, *SLA* is unrelated to unit-area photosynthetic rates (Wright *et al.* 2004, 2005). All else being equal, high *SLA* leads to lower H_v (Figs. 2 and 3). Hence, the compensation between K_s and H_v (keeping K_L constant) avoids high-*SLA* leaves experiencing lower stomatal conductance and lower unit-area photosynthetic rates. The general result is that high-*SLA* (or "acquisitive") leaves are necessarily associated with larger canopy areas (for a given investment in sapwood area), while an absolute increase in xylem K_s helps maintain hydraulic supply to the larger canopy (cf., SI Section 2).

While *SLA* values obtained from TRY may reflect conditions of partial canopy shading (Keenan & Niinemets 2016), this is unlikely to lead to different conclusions.

Overall, cross-species changes in H_v against either M_L or *SLA* are compensated for by changes in K_s. This is confirmed both by the scaling of H_v directly against K_s (negative isometry, i.e., b=-1.00, Table 1) and by the fact that the negative relationship between these two variables remains even after accounting for the covariance among traits (Figure 2). Therefore, covariation between H_v and K_s changes the cross-species balance between conductive areas and specific conductivity per unit area, maintaining similar levels of leaf hydraulic supply with varying *SLA* and M_L. The existence of a compensation between these two hydraulic properties has been reported already (Ewers & Fisher 1991; Martínez-Vilalta *et al.* 2004; Choat *et al.* 2011; Togashi *et al.* 2015), but its significance at the global scale had not been realised. While a trade-off between hydraulic efficiency and safety prevents the occurrence of plants with high efficiency and high safety (Gleason *et al.* 2016), the negative isometric scaling between xylem efficiency and H_v separates high relative allocation to a hydraulically inefficient xylem, versus low allocation to xylem with high hydraulic efficiency. This is similar to and likely overlaps with the trade-off generally observed across wood types, i.e., from tracheid-based conifer wood to diffuse-porous and ring-porous angiosperm wood. This compensation justifies a broadly constant leaf-specific hydraulic conductivity K_L with varying *SLA*, M_L, *WD* (cf., Table 1) and, as discussed later, plant stature.

The regulation of H_v by leaf and xylem traits takes place via different processes. In the case of *SLA*, the regulation is assured partly by the mathematical link between these two variables at constant leaf biomass investment (Lloyd *et al.* 2013; Osnas *et al.* 2013). The association between *SLA* and H_v therefore links water transport traits to the ecological trade-offs behind LES traits. In the case of M_L, the regulation occurs because changes in M_L inevitably lead to changes in total mass investment in leaves, although reductions in leaf numbers *n* partly compensate increases in M_L. Therefore, the M_L-H_v effect is mediated via the effect of Corner's rules on leaf packing (Smith *et al.* 2017). Finally, in the case of the regulation of H_v by K_s, a compensation takes place between investment in thick but inefficient versus thin but efficient xylem. From this perspective, Corner's rules, LES and hydraulic supply to leaves are largely decoupled axes of variation.

The role of plant stature

Plant stature is negatively correlated with H_v. If the relationship between stature and Huber values was determined by gravity or the need to counter frictional losses during water transport,

one would predict a positive effect (Eqn.2). Indeed, this is typically observed within species (i.e., when H_v changes during development at constant maximum height; McDowell *et al.* 2002). The occurrence of a negative isometric relationship suggests instead that stature brings about the need to reduce relative biomass allocation to sapwood, possibly as a consequence of sapwood carbon costs versus leaf gains (Mencuccini 2003; Niinemets 2010; Anfodillo *et al.* 2016; Fajardo *et al.* 2019). This may especially be the case under low light and/or high competitive conditions, where carbon balance may be less favourable (Togashi *et al.* 2015). Nonetheless, the correlation coefficient of H_{max} with H_v is lower than for almost all other traits (Table 1). Equivalently, the standardised coefficient for H_{max} is the lowest among the variables controlling changes in H_v in our path models (Figs. 2,3), suggesting that changes in stature are not strongly correlated with sapwood-leaf area ratios, when all the other variables are partialled out. This low correlation is likely caused by the covariation between H_{max} and other leaf traits and the compensation between H_v and K_s. In our path models, K_s is negatively related to H_v while it co-varies positively with H_{max}, hence net size effects of H_{max} on H_v are strongly reduced. Assuming a broadly constant H_v along a plant profile (Mencuccini *et al.* 2019), the negative isometric scaling (slope of -1.00, cf., Table 1) between H_v and H_{max} suggests that allocation to sapwood relative to leaf area for the whole plant is likely much less variable than indicated only by branch-top H_v, although datasets to test this hypothesis globally do not currently exist. Isometric scalings were also found for K_s against H_{max} (slope of +1.00) and H_v against K_s (slope of -1.00). Hence, a broadly constant branch-top leaf-specific hydraulic conductivity K_L is maintained (cf., West *et al.* 1999), despite the increasing stature of tall trees. This occurs *via* increases in specific conductivity (likely via increased canopy-top conduit diameters, Olson *et al.* 2014, 2018) and reductions in H_v, probably to avoid stature-related carbon costs (Mencuccini 2003). Plant stature also co-varies with M_L (and more weakly, *SLA*). Compared to shrubs (most of them, from desert or woodland, not boreal, biomes), tall (mainly tropical) trees are characterised by larger leaves and, less consistently, leaves with high specific leaf area. This also contrasts with trends occurring within individual trees, where leaf size and SLA strongly decline with height (Koch *et al.* 2004; Burgess & Dawson 2007).

The role of wood density

The negative association of *WD* with H_v is robust to the covariation with other organ-level traits, categorical and climatic variables. A mechanistic interpretation of the role of *WD* is complicated by its involvement in several processes (cf., discussion in Supplementary Materials Section S1). The direct negative effect of *WD* on H_v most likely reflects a bio-mechanical / carbon

cost trade-off between smaller but denser sapwood areas versus larger areas made up of cheaper wood, perhaps via the relationships between *WD* and wood mechanical properties (Chave *et al.* 2009; Niklas & Spatz 2010). *WD* also acts indirectly via conduit size and packing (which lead to negative covariance of *WD* with K_s, cf., derivation in SI, Section S1) and via its covariances with *SLA* and M_L. *WD* may also be linked to abundance of fibres, fibre wall thickness and parenchyma wood fractions (Ziemińska *et al.* 2015). We considered that *WD* may act on H_v via hydraulic safety. This analysis however shows no significant effect of P50 on H_v in a path model with the other traits (data not shown).

Climate and other moderating variables

Within species, H_v can respond to climatic conditions, e.g., radiation, site water balance, vapour pressure deficit and/or temperature (Mencuccini & Grace 1995; Delucia *et al.* 2000). We confirm these findings globally, with significant cross-species effects of MAT, MAP and MI on H_v. One of the most interesting results of our analysis is that direct climatic effects on H_v become non-significant or very small when the effects of MAT, MAP and especially of MI, are tested in a path model, accounting for indirect climatic effects via H_{max} and leaf/xylem traits. This finding suggests that evolutionary pressure by climate on H_v may largely occur via the component traits, e.g., reducing H_{max}, K_s, M_L and *SLA* under dry conditions.

Prediction of hydraulic traits for global models

Global models increasingly need to be parameterised with wood-to-leaf biomass ratios and hydraulic traits (Fatichi *et al.* 2016; Matheny *et al.* 2017; Mencuccini *et al.* 2019), including H_v and K_s specific to different plant functional types. However, adequate parameterisation of hydraulic and biomass scaling in terrestrial biosphere models requires understanding of how the relevant traits are integrated and co-vary with one another. A model for sapwood/leaf partitioning based entirely on organ-specific traits has the advantage of increasing model consistency and avoid over-parameterization. The fact that the model including only four easily measured and widely available traits (*SLA*, M_L, H_{max} and *WD*) performs similarly to the models including the less available xylem efficiency K_s raises the possibility that H_v may be estimated globally from parameters already employed in models. Additionally, the negative isometric scaling between H_v and K_s is robust to several comparisons across potential grouping variables and to the covariation with other traits.

Therefore, it may also be possible to predict K_s as a function of H_v, assuming a globally constant K_L. Further investigations are required to determine the robustness of this approach for modelling hydraulic traits in different plant functional types.

Our conclusion that relative partitioning to sapwood/leaf area can be explained via component traits is limited to the canopy-top branches where H_v was measured. Using the limited available data, Mencuccini *et al.* (2019) showed that, while varying from species to species, H_v tend to remain relatively constant from twig to trunk base. A constant sapwood-leaf ratio along the plant axis is consistent with metabolic scaling theory (West *et al.* 1999; Savage *et al.* 2010). However, neither the dataset we previous employed (Mencuccini *et al.* 2019), nor metabolic scaling theory account for light-dependent variation in traits within tree canopies.

About 40% of the variance in H_v remains unaccounted for in our models. Part of this variance could be explained by variations in the factor K_p/n, which is incorporated in Eqn. 2 but is not quantified due to lack of data. Similarly, lack of size (A_x, distance from apex, sampling height) measurements prevent us from investigating additional constraints, such as axial variability in K_s. Methodological uncertainties for K_s (e.g., Espino & Schenk 2011) and study-to-study variability in the sampling strategy for H_v (leaf and xylem phenology; infrequent use of dyes) add to the same problem. A better understanding of H_v scaling within plants is essential to estimate how leaf/wood partitioning can be scaled from branches to whole plants (Mencuccini *et al.* 2019).

Acknowledgements

This research was supported by the Spanish Ministry of Economy and Competitiveness (MINECO) via competitive grants CGL2013-46808-R (FUN2FUN project) and CGL2017-89149-C2-1-R (DRESS project). T.R. was supported by a FPI scholarship from the MINECO. J.M.V. benefited from an ICREA Academia award. FS acknowledges support from a University of Nottingham Anne McLaren fellowship. The study was supported by the TRY initiative on plant traits (http://www.try-db.org). We thank S Patiño (deceased) and J Lloyd for initially drawing our attention to the RAINFOR and TROBIT field collections of Huber values. The data derived from the hydraulics database is partly an outcome from a working group funded by the ARC through the Australia–New Zealand Research Network for Vegetation Function.

Reference List

Anfodillo, T., Carraro, V., Carrer, M., Fior, C. & Rossi, S. (2006). Convergent tapering of xylem conduits in different woody species. *New Phytol.*, 169, 279–290.

Anfodillo, T., Petit, G., Sterck, F., Lechthaler, S. & Olson, M.E. (2016). Allometric trajectories and "stress": A quantitative approach. *Front. Plant Sci.*, 7, 1–6.

Bloom, A.J., Chapin, S.F. & Mooney, H.A. (1985). Resource limitation in plants- An economic analogy. *Annu. Rev. Ecol. Syst.*

Brodribb, T.J., Holbrook, N.M., Zwieniecki, M.A. & Palma, B. (2004). Leaf hydraulic capacity in ferns, conifers and angiosperms: impacts on photosynthetic maxima. *New Phytol.*, 165, 839–846.

Brown, T.A. (2006). *Confirmatory Factor Analysis for Applied Research*. *Methodol. Soc. Sci.*

Burgess, S.S.O. & Dawson, T.E. (2007). Predicting the limits to tree height using statistical regression of leaf traits. *New Phytol.*, 174, 626–636.

Cayuela, L., Granzow-de la Cerda, Í., Albuquerque, F.S. & Golicher, D.J. (2012). taxonstand: An r package for species names standardisation in vegetation databases. *Methods Ecol. Evol.*, 3, 1078–1083.

Chave, J., Coomes, D., Jansen, S., Lewis, S.L., Swenson, N.G. & Zanne, A.E. (2009). Towards a worldwide wood economics spectrum. *Ecol. Lett.*, 12, 351–366.

Choat, B., Jansen, S., Brodribb, T.J., Cochard, H., Delzon, S., Bhaskar, R., *et al.* (2012). Global convergence in the vulnerability of forests to drought. *Nature*, 491, 752–755.

Choat, B., Medek, D.E., Stuart, S.A., Pasquet-Kok, J., Egerton, J.J.G., Salari, H., *et al.* (2011). Xylem traits mediate a trade-off between resistance to freeze-thaw-induced embolism and photosynthetic capacity in overwintering evergreens. *New Phytol.*, 191, 996–1005.

Coleman, J.S., McConnaughay, K.D.M. & Ackerly, D.D. (1994). Interpreting phenotypic variation in plants. *Trends Ecol. Evol.*, 9, 186.

Corner, E.J.H. (1949). The Durian theory or the origin of the modern tree. *Ann. Bot.*, 13, 367–414.

Delucia, E.H., Maherali, H. & Carey, E. V. (2000). Climate-driven changes in biomass allocation in pines. *Glob. Chang. Biol.*, 6, 587–593.

Dewar, R.C., Franklin, O., Mäkelä, A., McMurtrie, R.E. & Valentine, H.T. (2009). Optimal function explains forest responses to global change. *Bioscience*, 59, 127–139.

Duursma, R.A. & Falster, D.S. (2016). Leaf mass per area, not total leaf area, drives differences in above-ground biomass distribution among woody plant functional types. *New Phytol.*, 212, 368–376.

Enquist, B.J. & Niklas, K.J. (2002). Global allocation rules for patterns of biomass partitioning in seed plants. *Science (80-.).*, 295, 1517–1520.

Espino, S. & Schenk, H.J. (2011). Mind the bubbles: Achieving stable measurements of maximum hydraulic conductivity through woody plant samples. *J. Exp. Bot.*, 62, 1119–1132.

Ewers, F.W. & Fisher, J.B. (1991). Why vines have narrow stems: histological trends in Bauhimia (Fabaceae). *Oecologia*, 88, 233–237.

Fajardo, A., McIntire, E.J.B. & Olson, M.E. (2019). When short stature is an asset in trees. *Trends Ecol.*

Evol., 34, 193–199.

Farrior, C.E., Dybzinski, R., Levin, S.A. & Pacala, S.W. (2013). Competition for Water and Light in Closed-Canopy Forests: A Tractable Model of Carbon Allocation with Implications for Carbon Sinks. *Am. Nat.*, 181, 314–330.

Fatichi, S., Pappas, C. & Ivanov, V.Y. (2016). Modeling plant-water interactions: an ecohydrological overview from the cell to the global scale. *Wiley Interdiscip. Rev. Water*, 3, 327–368.

Franklin, O., Johansson, J., Dewar, R.C., Dieckmann, U., McMurtrie, R.E., Brannstrom, A., *et al.* (2012). Modeling carbon allocation in trees: a search for principles. *Tree Physiol.*, 32, 648–666.

Freschet, G.T., Valverde-Barrantes, O.J., Tucker, C.M., Craine, J.M., McCormack, M.L., Violle, C., *et al.* (2017). Climate, soil and plant functional types as drivers of global fine-root trait variation. *J. Ecol.*, 105, 1182–1196.

Gill, R.A. & Jackson, R.B. (2000). Global patterns of root turnover for terrestrial ecosystems. *New Phytol.*, 147, 13–31.

Gleason, S.M., Butler, D.W., Ziemińska, K., Waryszak, P. & Westoby, M. (2012). Stem xylem conductivity is key to plant water balance across Australian angiosperm species. *Funct. Ecol.*, 26, 343–352.

Gleason, S.M., Westoby, M., Jansen, S., Choat, B., Hacke, U.G., Pratt, R.B., *et al.* (2016). Weak tradeoff between xylem safety and xylem-specific hydraulic efficiency across the world's woody plant species. *New Phytol.*, 209, 123–136.

Grime, J.P. (1979). *Plant Strategies and Vegetation Processes*. John Wiley and Sons, New York.

Hacke, U.G., Sperry, J.S., Pockman, W.T., Davis, S.D. & McCulloh, K.A. (2001). Trends in wood density and structure are linked to prevention of xylem implosion by negative pressure. *Oecologia*, 126, 457–461.

Hunt, R. & Cornelissen, J.H.C.C. (1997). Components of relative growth rate and their interrelations in 59 temperate plant species. *New Phytol.*, 135, 395–417.

Kattge, J., Diaz, S., Lavorel, S., Prentice, I.C., Leadley, P., Bonisch, G., *et al.* (2011). TRY - a global database of plant traits. *Glob. Chang. Biol.*, 17, 2905–2935.

Keenan, T.F. & Niinemets, Ü. (2016). Global leaf trait estimates biased due to plasticity in the shade. *Nat. Plants*, 3.

Kikuzawa, K. (1991). A cost-benefit analysis of leaf habit and leaf longevity of trees and their geographical pattern. *Am. Nat.*, 138, 1250–1263.

Kleiman, D. & Aarssen, L.W. (2007). The leaf size/number trade-off in trees. *J. Ecol.*, 95, 376–382.

Koch, G.W., Sillet, S.C., Jennings, G.M. & Davis, S.D. (2004). The limits to tree height. *Nature*, 428, 851–854.

Lapenis, A., Shvidenko, A., Shepaschenko, D., Nilsson, S. & Aiyyer, A. (2005). Acclimation of Russian forests to recent changes in climate. *Glob. Chang. Biol.*, 11, 2090–2102.

Ledo, A., Paul, K.I., Burslem, D.F.R.P., Ewel, J.J., Barton, C., Battaglia, M., *et al.* (2017). Tree size and climatic water deficit control root to shoot ratio in individual trees globally. *New Phytol.*, 217, 8–11.

Liu, H., Gleason, S.M., Hao, G., Hua, L., He, P., Goldstein, G., *et al.* (2019). Hydraulic traits are coordinated with maximum plant height at the global scale. *Sci. Adv.*, 5, eaav1332.

Lloyd, J., Bloomfield, K., Domingues, T.F. & Farquhar, G.D. (2013). Photosynthetically relevant foliar traits correlating better on a mass vs an area basis: of ecophysiological relevance or just a case of mathematical imperatives and statistical quicksand? *New Phytol.*, 199, 311–321.

Martínez-Vilalta, J., Sala, A. & Piñol, J. (2004). The hydraulic architecture of Pinaceae – a review. *Plant Ecol.*, 171, 3–13.

Matheny, A.M., Mirfenderesgi, G. & Bohrer, G. (2017). Trait-based representation of hydrological functional properties of plants in weather and ecosystem models. *Plant Divers.*, 39, 1–12.

McCarthy, M.C. & Enquist, B.J. (2007). Consistency between an allometric approach and optimal partitioning theory in global patterns of plant biomass allocation. *Funct. Ecol.*, 21, 713–720.

McDowell, N., Barnard, H., Bond, B.J., Hinckley, T., Hubbard, R.M., Ishii, H., *et al.* (2002). The relationship between tree height and leaf area: Sapwood area ratio. *Oecologia*, 132, 12–20.

Meinzer, F.C., Brooks, J.R., Bucci, S., Goldstein, G., Scholz, F.G. & Warren, J.M. (2004). Converging patterns of uptake and hydraulic redistribution of soil water in contrasting woody vegetation types. *Tree Physiol.*, 24, 919–28.

Mencuccini, M. (2002). Hydraulic constraints in the functional scaling of trees. *Tree Physiol.*, 22, 553–565.

Mencuccini, M. (2003). The ecological significance of long-distance water transport: short-term regulation, long-term acclimation and the hydraulic costs of stature across plant life forms. *Plant. Cell Environ.*, 26, 163–182.

Mencuccini, M. & Grace, J. (1995). Climate influences the leaf area/sapwood area ratio in Scots pine. *Tree Physiol.*, 15, 1–10.

Mencuccini, M., Manzoni, S. & Christoffersen, B. (2019). Modelling water fluxes in plants: from tissues to biosphere. *New Phytol.*, 222.

Mitchell, P.J., Veneklaas, E.J., Lambers, H. & Burgess, S.S.O. (2008). Using multiple trait associations to define hydraulic functional types in plant communities of south-western Australia. *Oecologia*, 158, 385–397.

Niinemets, Ü. (1999). Components of leaf dry mass per area - thickness and density - alter leaf photosynthetic capacity in reverse directions in woody plants. *New Phytol.*, 144, 35–47.

Niinemets, Ü. (2001). Global-scale climatic controls of leaf dry mass per area, density, and thickness in trees and shrubs. *Ecology*, 82, 453–469.

Niinemets, Ü. (2010). A review of light interception in plant stands from leaf to canopy in different plant functional types and in species with varying shade tolerance. *Ecol. Res.*, 25, 693–714.

Niinemets, Ü., Keenan, T.F. & Hallik, L. (2015). A worldwide analysis of within-canopy variations in leaf structural, chemical and physiological traits across plant functional types. *New Phytol.*, 205, 973–993.

Niinemets, Ü., Portsmuth, A., Tena, D., Tobias, M., Matesanz, S. & Valladares, F. (2007). Do we underestimate the importance of leaf size in plant economics? Disproportional scaling of support costs within the spectrum of leaf physiognomy. *Ann. Bot.*, 100, 283–303.

Niklas, K.J. & Spatz, H.C. (2006). Allometric theory and the mechanical stability of large trees: Proof and conjecture. *Am. J. Bot.*, 93, 824–828.

Niklas, K.J. & Spatz, H.C. (2010). Worldwide correlations of mechanical properties and green wood

667 density. *Am. J. Bot.*, 97, 1587–1594.

668 Niu, C.-Y., Meinzer, F.C. & Hao, G.-Y. (2017). Divergence in strategies for coping with winter
669 embolism among co-occurring temperate tree species: the role of positive xylem pressure,
670 wood type and tree stature. *Funct. Ecol.*, 31, 1550–1560.

671 Olson, M.E., Aguirre-Hernández, R. & Rosell, J.A. (2009). Universal foliage-stem scaling across
672 environments and species in dicot trees: Plasticity, biomechanics and Corner's Rules. *Ecol. Lett.*,
673 12, 210–219.

674 Olson, M.E., Anfodillo, T., Rosell, J.A., Petit, G., Crivellaro, A., Isnard, S., *et al.* (2014). Universal
675 hydraulics of the flowering plants: Vessel diameter scales with stem length across angiosperm
676 lineages, habits and climates. *Ecol. Lett.*, 17, 988–997.

677 Olson, M.E., Soriano, D., Rosell, J.A., Anfodillo, T., Donoghue, M.J., Edwards, E.J., *et al.* (2018). Plant
678 height and hydraulic vulnerability to drought and cold. *Proc. Natl. Acad. Sci. USA*, 115, 7551–
679 7556.

680 Osnas, J.L.D., Lichstein, J.W., Reich, P.B. & Pacala, S.W. (2013). Global leaf trait relationships: Mass,
681 area, and the leaf economics spectrum. *Science (80-.).*, 340, 741–744.

682 Patiño, S. (2005). *Manual de campo para el estudio de hojas y madera editado para establecer*
683 *efectos de sequías*. Proyecto Pan-Amazonia, EU, 12 pp.

684 Patiño, S., Fyllas, N.M., Baker, T.R., Paiva, R., Quesada, C.A., Santos, A.J.B., *et al.* (2012). Coordination
685 of physiological and structural traits in Amazon forest trees. *Biogeosciences*, 9, 775–801.

686 Pickup, M., Westoby, M. & Basden, A. (2005). Dry mass costs of deploying leaf area in relation to leaf
687 size. *Funct. Ecol.*, 19, 88–97.

688 Pinheiro, J.C. & Bates, D.M. (2000). *Mixed-Effects Models in S and S-PLUS*. Springer-Verlag New York
689 Berlin Heidelberg.

690 Poorter, H., Jagodzinski, A.M., Ruiz-Peinado, R., Kuyah, S., Luo, Y., Oleksyn, J., *et al.* (2015). How does
691 biomass distribution change with size and differ among species? An analysis for 1200 plant
692 species from five continents. *New Phytol.*, 208, 736–749.

693 Poorter, H., Niklas, K.J., Reich, P.B., Oleksyn, J., Poot, P. & Mommer, L. (2012). Biomass allocation to
694 leaves, stems and roots: meta-analysis of interspecific variation and environmental control.
695 *New Phytol.*, 193, 30–50.

696 R Core Team. (2017). R: A language and environment for statistical computing.

697 Reich, P.B. (2002). Root–shoot relations: optimality in acclimation and adaptation or the. 'Emperor's
698 New Clothes'? In: *Plant Roots: The Hidden Half* (eds. Waisel, Y., Amram, E. & Kafkafi, U.).
699 Marcel Dekker, New York, pp. 205–220.

700 Reich, P.B., Luo, Y., Bradford, J.B., Poorter, H., Perry, C.H. & Oleksyn, J. (2014a). Temperature drives
701 global patterns in forest biomass distribution in leaves, stems, and roots. *Proc. Natl. Acad. Sci.*
702 *U. S. A.*, 111, 13721–13726.

703 Reich, P.B., Rich, R.L., Lu, X., Wang, Y.-P. & Oleksyn, J. (2014b). Biogeographic variation in evergreen
704 conifer needle longevity and impacts on boreal forest carbon cycle projections. *Proc. Natl.*
705 *Acad. Sci. U. S. A.*, 111, 13703–13708.

706 Reich, P.B., Walters, M.B. & Ellsworth, D.S. (1997). From tropics to tundra: Global convergence in
707 plant functioning. *Proc. Natl. Acad. Sci. U. S. A.*, 94, 13730–13734.

Rosseel, Y. (2012). lavaan: An R Package for Structural Equation Modeling. *J. Stat. Softw.*, 48, 1–36.

Santiago, L.S., Goldstein, G., Meinzer, F.C., Fisher, J.B., Machado, K., Woodruff, D., *et al.* (2004). Leaf photosynthetic traits scale with hydraulic conductivity and wood density in Panamanian forest canopy trees. *Oecologia*, 140, 543–550.

Savage, V.M., Bentley, L.P., Enquist, B.J., Sperry, J.S., Smith, D.D., Reich, P.B., *et al.* (2010). Hydraulic trade-offs and space filling enable better predictions of vascular structure and function in plants. *Proc. Natl. Acad. Sci. USA*, 107, 22722–7.

Schrodt, F., Domingues, T.F., Feldpausch, T.R., Saiz, G., Quesada, C.A., Schwarz, M., *et al.* (2015). Foliar trait contrasts between African forest and savanna trees: Genetic versus environmental effects. *Funct. Plant Biol.*, 42, 63–83.

Scoffoni, C., Chatelet, D.S., Pasquet-kok, J., Rawls, M., Donoghue, M.J., Edwards, E.J., *et al.* (2016). Hydraulic basis for the evolution of photosynthetic productivity. *Nat. Plants*, 2, 16072.

Shipley, B. (2006). Net assimilation rate, specific leaf area and leaf mass ratio: Which is most closely correlated with relative growth rate? A meta-analysis. *Funct. Ecol.*, 20, 565–574.

Shipley, B., Lechowicz, M.J., Wright, I. & Reich, P.B. (2006). Fundamental trade-offs generating the worldwide leaf economics spectrum. *Ecology*, 87, 535–541.

Smith, D.D., Sperry, J.S. & Adler, F.R. (2017). Convergence in leaf size versus twig leaf area scaling: do plants optimize leaf area partitioning? *Ann. Bot.*, 119, 447–456.

Song, J., Yang, D., Niu, C.-Y., Zhang, W.-W., Wang, M. & Hao, G.-Y. (2018). Correlation between leaf size and hydraulic architecture in five compound-leaved tree species of a temperate forest in NE China. *For. Ecol. Manage.*, 418, 63–72.

Stratton, L., Goldstein, G. & Meinzer, F.C. (2000). Stem water storage capacity and efficiency of water transport: their functional significance in a Hawaiian dry forest. *Plant, Cell Environ.*, 23, 99–106.

Thornley, J.H.M. (1972). A balanced quantitative model for root:shoot ratios in vegetative plants. *Ann. Bot.*, 36, 431–441.

Tilman, D. (1988). *Plant Strategies and the Dynamics and Structure of Plant Communities*. Princeton University Press, Princeton, NJ, USA, 376 pp.

Togashi, H.F., Prentice, I.C., Evans, B.J., Forrester, D.I., Drake, P., Feikema, P., *et al.* (2015). Morphological and moisture availability controls of the leaf area-to-sapwood area ratio: analysis of measurements on Australian trees. *Ecol. Evol.*, 5, 1263–1270.

Trabucco, A., Zomer, R.J., Bossio, D.A., van Straaten, O. & Verchot, L. V. (2008). Climate change mitigation through afforestation/reforestation: A global analysis of hydrologic impacts with four case studies. *Agric. Ecosyst. Environ.*, 126, 81–97.

Tyree, M.T. & Ewers, F.W. (1991). The hydraulic architecture of trees and other woody plants. *New Phytol.*, 119, 345–360.

Warton, D.I., Wright, I.J., Falster, D.S. & Westoby, M. (2006). Bivariate line-fitting methods for allometry. *Biol. Rev.*, 81, 259–291.

West, G.B., Brown, J.H. & Enquist, B.J. (1999). A general model for the structure and allometry of plant vascular systems. *Nature*, 400, 664–667.

Westoby, M. (1998). A leaf–height–seed (LHS) plant ecology strategy scheme. *Plant Soil*, 199, 213–

227.

Westoby, M. & Wright, I.J. (2003). The leaf size – twig size spectrum and its relationship to other important spectra of variation among species. *Oecologia*, 135, 621–628.

Whitehead, D. & Jarvis, P.G. (1981). Coniferous forests and plantations. In: *Water Deficits and Plant Growth* (ed. Kozlowski, T.T.). Academic Press, New York, pp. 49–152.

Wright, I.J., Dong, N., Maire, V., Prentice, I.C., Westoby, M., Díaz, S., *et al.* (2017). Global climatic drivers of leaf size. *Science (80-.).*, 357, 917–921.

Wright, I.J., Reich, P.B., Cornelissen, J.H.C., Falster, D.S., Garnier, E., Hikosaka, K., *et al.* (2005). Assessing the generality of global leaf trait relationships. *New Phytol.*, 166, 485–496.

Wright, I.J., Reich, P.B., Westoby, M., Ackerly, D.D., Baruch, Z., Bongers, F., *et al.* (2004). The worldwide leaf economics spectrum. *Nature*, 428, 821–827.

Wu, J., Albert, L.P., Lopes, A.P., Restrepo-Coupe, N., Hayek, M., Wiedemann, K.T., *et al.* (2016). Leaf development and demography explain photosynthetic seasonality in Amazon evergreen forests. *Science (80-.).*, 351, 972–976.

Zanne, A.E., Tank, D.C., Cornwell, W.K., Eastman, J.M., Smith, S.A., Fitzjohn, R.G., *et al.* (2014). Three keys to the radiation of angiosperms into freezing environments. *Nature*, 506, 89–92.

Zhu, S.-D., Song, J.-J., Li, R.-H. & Ye, Q. (2013). Plant hydraulics and photosynthesis of 34 woody species from different successional stages of subtropical forests. *Plant. Cell Environ.*, 36, 879–891.

Ziemińska, K., Westoby, M. & Wright, I.J. (2015). Broad anatomical variation within a narrow wood density range—A study of twig wood across 69 Australian angiosperms. *PLoS One*, 10, e0124892.

Zimmermann, M.H. (1983). *Xylem Structure and the Ascent of Sap*. Springer, Berlin Heidelberg.

774 Table 1. Results of Standardised Major Axis analyses of the bivariate relationships among the plant
775 traits affecting H_v. All variables are base-10 log-transformed. Formulas are given as: $X_2=f(X_1)$. Legend:
776 CI, confidence intervals; H_v, Huber value; *SLA*, Specific Leaf Area; A_L, leaf area; M_L, leaf mass; K_s,
777 xylem specific conductivity; H_{max}, maximum plant height; *WD*, wood density. Sample size (n),
778 correlation coefficient (r) and probability level (P value) for each regression are also given.

X_2	X_1	Y-Intercept	95% CI of the elevation	Slope (95% CI)	95% CI of the slope	n	|r|	(P value)
H_v	*SLA*	2.126	2.021 / 2.231	-1.934	-2.041 / -1.833	1039	0.60	$<2.2\ e^{-16}$
H_v	A_L	0.874	0.824 / 0.923	-0.442	-0.470 / -0.416	822	0.60	$<2.2\ e^{-16}$
H_v	M_L	0.459	0.422 / 0.497	-0.497	-0.532 / -0.464	780	0.54	$<2.2\ e^{-16}$
H_v	K_s	0.481	0.432 / 0.531	-1.039	-1.126 / -0.960	448	0.53	$<2.2\ e^{-16}$
H_v	H_{max}	1.413	1.339 / 1.486	-0.963	-1.021 / -0.908	798	0.45	$<2.2\ e^{-16}$
H_v	*WD*	1.118	1.045 / 1.192	1.721	1.608 / 1.842	1018	0.06	0.09
K_s	*SLA*	-1.300	-1.450 / -1.151	1.601	1.458 / 1.758	397	0.35	$4.9\ e^{-12}$
K_s	A_L	-0.326	-0.415 / -0.236	0.494	0.438 / 0.557	218	0.48	$2.5\ e^{-13}$
K_s	M_L	0.145	0.075 / 0.215	0.557	0.492 / 0.632	208	0.45	$2.0\ e^{-11}$
K_s	*WD*	-0.667	-0.774 / -0.560	-1.673	-1.845 / -1.514	386	0.18	0.0006
K_s	H_{max}	-0.879	-0.994 / -0.764	1.004	0.913 / 1.104	316	0.30	$7.1\ e^{-8}$
M_L	*SLA*	-3.622	-3.943 / -3.300	4.101	3.802 / 4.424	780	0.30	$8.8\ e^{-14}$
M_L	A_L	-0.869	-0.896 / -0.842	0.911	0.896 / 0.927	780	0.98	$<2.2\ e^{-16}$
M_L	*WD*	-1.019	-1.170 / -0.867	-3.022	-3.277 / -2.787	746	0.18	$2.5\ e^{-5}$
M_L	H_{max}	-2.276	-2.481 / -2.071	2.173	2.026 / 2.330	598	0.48	$<2.2\ e^{-16}$
SLA	A_L	0.676	0.674 / 0.705	0.222	0.207 / 0.238	802	0.44	$<2.2\ e^{-16}$
SLA	*WD*	0.477	0.438 / 0.516	-0.956	-1.021 / -0.894	976	0.29	$6.4\ e^{-16}$
SLA	H_{max}	0.323	0.277 / 0.369	0.539	0.505 / 0.575	754	0.38	$<2.2\ e^{-16}$
WD	A_L	-0.060	-0.105 / -0.015	-0.296	-0.320 / -0.273	759	0.20	$9.3\ e^{-7}$
WD	H_{max}	0.236	0.179 / 0.293	-0.609	-0.652 / -0.569	722	0.23	$2.4\ e^{-10}$
A_L	H_{max}	-1.369	-1.568 / -1.169	2.260	2.116 / 2.414	638	0.53	$<2.2\ e^{-16}$

779

780

781 **Figure legends.**

782 **Figure 1.** Bivariate plots of Huber Value H_v against other plant traits, i.e., A) specific leaf area (*SLA*),
783 B) plant stature (H_{max}), C) leaf mass (M_L) and D) xylem specific conductivity (K_s). All variables are
784 base-10 log-transformed. Points are coloured to distinguish Gymnosperms (black triangles) from
785 Angiosperms (circles), and among these, trees (red circles) from shrubs (blue circles). The thin black
786 line gives the overall model II regression scaling across all data points (cf., Table 1). Thick black, blue
787 and red lines give separate scaling for the three respective groups. Statistics of the regressions and
788 the comparisons among groups (shrub vs. trees; Angiosperms vs. Gymnosperms) are given in Table
789 S1.

790 **Figure 2.** Results of the Path models explaining Huber Value (H_v) based on A) specific leaf area (*SLA*),
791 leaf mass (M_L), plant stature (H_{max}) and xylem specific conductivity (K_s) or B) the same variables plus
792 wood density (*WD*). Data from both angiosperms and gymnosperms are included. All variables are
793 base-10 log-transformed. All coefficients are standardised. Green single-headed lines (and respective
794 numbers) indicate positive relationships, red single-headed lines (and numbers), negative
795 relationships (from cause to effect). Double-headed arrows (and numbers) indicate covariances
796 among variables. The thicknesses of the lines are proportional to the intensity of the effect. Green
797 numbers close to the rounded arrows around each rectangle give the proportion of unexplained
798 variance for each model (values of 1 are given for the predictor variables). The difference between
799 observed and modelled covariance structure is not significant in either of the two models based on a
800 chi-square test (P=0. 697 and P=0. 727, respectively).

801 **Figure 3.** Results of the Path model explaining Huber Value (H_v) based on specific leaf area (*SLA*),
802 individual leaf mass (M_L), plant stature (H_{max}) and wood density (*WD*). All variables are base-10 log-
803 transformed. All coefficients are standardised. Green single-headed lines (and respective numbers)
804 indicate positive relationships, red single-headed lines (and numbers), negative relationships (from
805 cause to effect). Double-headed arrows (and numbers) indicate covariances among variables. The
806 thicknesses of the lines are proportional to the intensity of the effect. Green numbers close to the
807 rounded arrows around each rectangle give the proportion of unexplained variance for each model
808 (values of 1 are given for the predictor variables). The difference between observed and modelled
809 covariance structure is not significant based on a chi-square test (P=0.469).

810

811

812

813

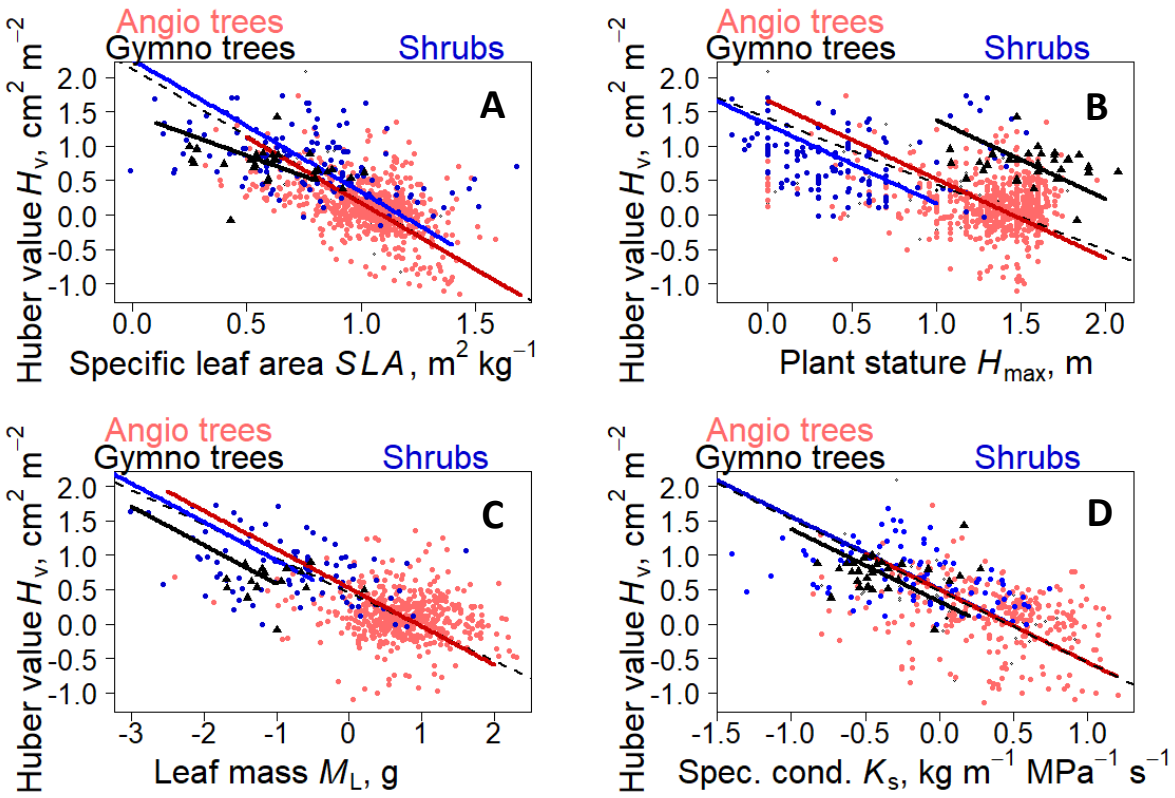

814

815 **Figure 1.** Bivariate plots of Huber Value H_v against other plant traits, i.e., A) specific leaf area (*SLA*),
816 B) plant stature (H_{max}), C) leaf mass (M_L) and D) xylem specific conductivity (K_s). All variables are
817 base-10 log-transformed. Points are coloured to distinguish Gymnosperms (black triangles) from
818 Angiosperms (circles), and among these, trees (red circles) from shrubs (blue circles). The thin black
819 line gives the overall model II regression scaling across all data points. Thick black, blue and red lines
820 give separate scaling for the three respective groups. Statistics of the regressions and the
821 comparisons among groups (shrub vs. trees; Angiosperms vs. Gymnosperms) are given in Tables 1
822 and S1.

823

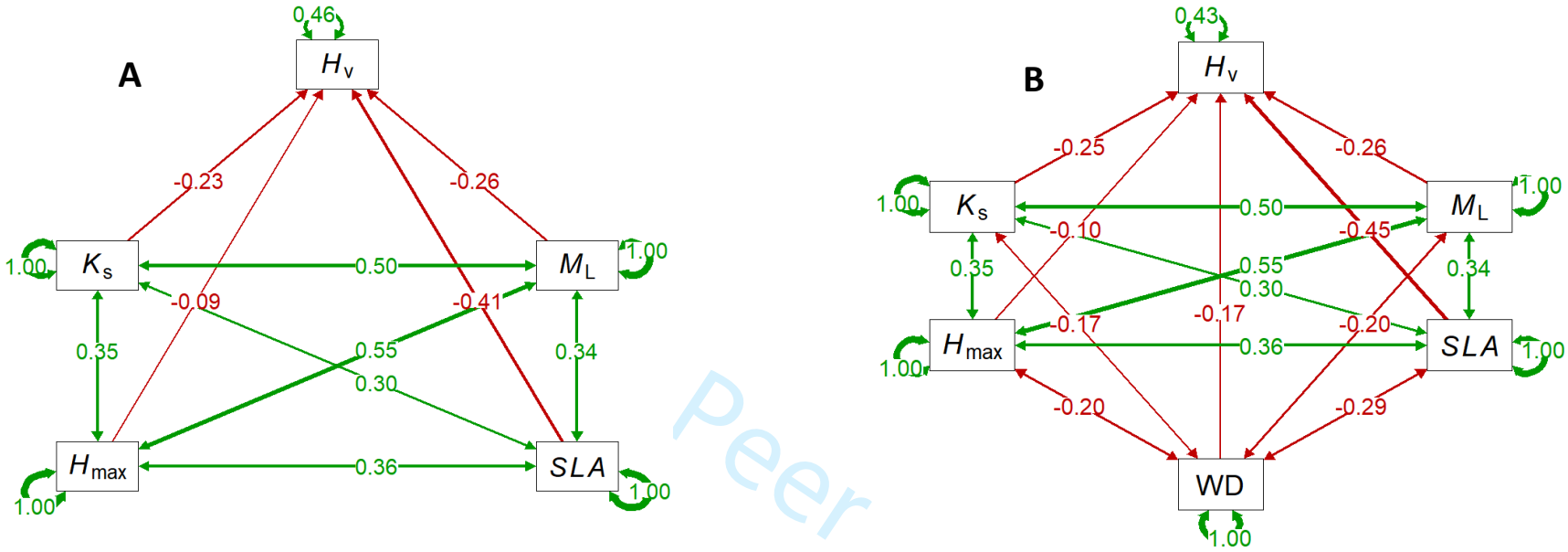

Figure 2. Results of the Path models explaining Huber Value (H_v) based on A) specific leaf area (*SLA*), leaf mass (M_L), plant stature (H_{max}) and xylem specific conductivity (K_s) or B) the same variables plus wood density (*WD*). Data from both angiosperms and gymnosperms are included. All variables are base-10 log-transformed. All coefficients are standardised. Green single-headed lines (and respective numbers) indicate positive relationships, red single-headed lines (and numbers), negative relationships (from cause to effect). Double-headed arrows (and numbers) indicate covariances among variables. The thicknesses of the lines are proportional to the intensity of the effect. Green numbers close to the rounded arrows around each rectangle give the proportion of unexplained variance for each model (values of 1 are given for the predictor variables). The difference between observed and modelled covariance structure is not significant in either of the two models based on a chi-square test (P=0. 697 and P=0. 727, respectively).

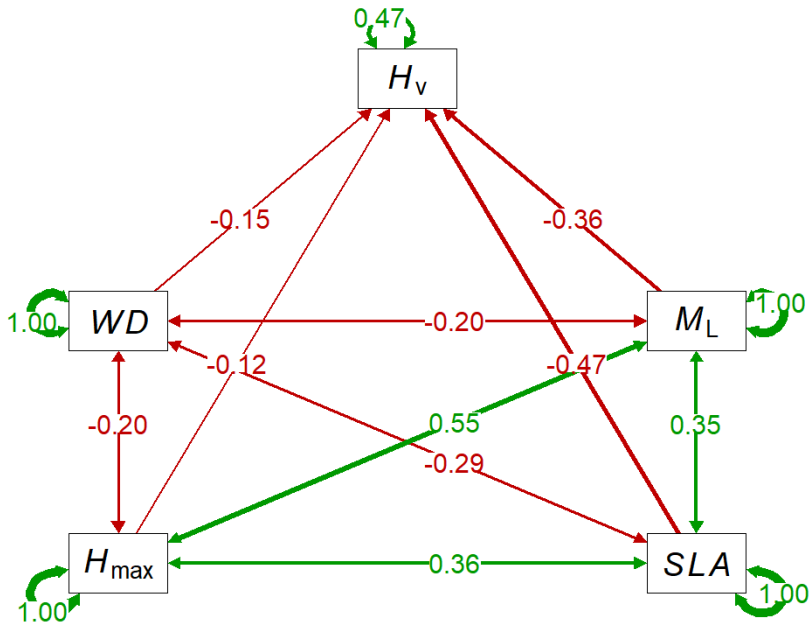

Figure 3. Results of the Path model explaining Huber Value (H_v) based on specific leaf area (*SLA*), individual leaf mass (M_L), plant stature (H_{max}) and wood density (*WD*). All variables are base-10 log-transformed. All coefficients are standardised. Green single-headed lines (and respective numbers) indicate positive relationships, red single-headed lines (and numbers), negative relationships (from cause to effect). Double-headed arrows (and numbers) indicate covariances among variables. The thicknesses of the lines are proportional to the intensity of the effect. Green numbers close to the rounded arrows around each rectangle give the proportion of unexplained variance for each model (values of 1 are given for the predictor variables). The difference between observed and modelled covariance structure is not significant based on a chi-square test (P=0.469).